Engineering Analysis with Boundary Elements 34 (2010) 625–631

Contents lists available at ScienceDirect

Engineering Analysis with Boundary Elements

journal homepage: www.elsevier.com/locate/enganabound

The comparison of three meshless methods using radial basis functions for solving fourth-order partial differential equations

Guangming Yao [a], C.H. Tsai [a], Wen Chen [b,*]

[a] Department of Mathematics, University of Southern Mississippi, Hattiesburg, MS 39406, USA
[b] Department of Mechanics, Hohai University, Nanjing, China

ARTICLE INFO

Article history:
Received 25 December 2009
Accepted 12 March 2010
Available online 3 April 2010

Keywords:
Radial basis function
MFS
MPS
Kansa's method

ABSTRACT

In this paper we apply the newly developed method of particular solutions (MPS) and one-stage method of fundamental solutions (MFS-MPS) for solving fourth-order partial differential equations. We also compare the numerical results of these two methods to the popular Kansa's method. Numerical results in the 2D and the 3D show that the MFS-MPS outperformed the MPS and Kansa's method. However, the MPS and Kansa's method are easier in terms of implementation.

1. Introduction

During the past two decades, radial basis functions (RBFs) have played an important role in the development of meshless methods for solving partial differential equations [2,3,8,10]. Kansa's method [10] is a well-known meshless method using RBFs. Due to its simplicity and effectiveness, Kansa's method has become very popular in the area of science and engineering. Meanwhile, another important development using RBFs is the extension of the method of fundamental solutions (MFS) for solving inhomogeneous equations [8,11]. In this approach, RBFs have been used to approximate the particular solution of the given governing equation. As a result of the approximate particular solution, the original inhomogeneous equation has been converted to a homogeneous equation. The MFS or other boundary methods are used to solve this homogeneous solution. This is a two-stage numerical scheme. In [13], a numerical comparison of these two approaches can be found where the numerical accuracy of these two approaches are similar. However, Kansa's method has the advantage of being able to solve partial differential equations with variable coefficients while the two-stage MFS cannot.

Recently, a one-stage numerical scheme using the MFS and RBFs has been proposed to further improve the MFS for solving partial differential equations with variable coefficients [1,17]. In this one-stage approach, the fundamental solution and the particular solution using RBFs have been used as two basis functions to directly approximate the given partial differential equation. The one-stage numerical scheme is called the MFS-MPS. One important aspect of this one-stage approach is that the MFS is capable of solving PDEs with variable coefficients. Thus competitive to Kansa's method. Followed by this development, two independent research groups [12,18] proposed to further improve the one-stage MFS by omitting the basis function of fundamental solution and using the particular solution of RBFs based basis function only to approximate the differential equation, this particular solution satisfied the boundary conditions. This numerical scheme is called the MPS. The MPS is somewhat similar to Kansa's method. As we shall see, when the radial basis functions r^{2n-1} are used, then the MPS and Kansa's method become identical. On the other hand, fourth-order partial differential equations are often encountered in many science and engineering problems [4,5,16], such as image processing for noise removal, ice formation [14], high-order plate theory, and some systems involving several second order elliptic equations. By the Hörmander operator decomposition technique [9], these coupled systems, such as a multiple porosity system or a multilayered aquifer system [6,7], can be reduced to a single higher order partial differential equations. It is meaningful to have a fair comparison between Kansa's method and newly developed MFS-MPS and MPS. The work in this paper is considered with fourth-order differential equations.

The organization of the paper is as follows. In Section 2, the type of partial differential equations with various kinds of boundary conditions is listed. In Section 3, we briefly introduce the method of particular solutions. In Section 4, we introduce the one-stage MFS-MPS. In Section 5, for completeness, we briefly introduce Kansa's method. In Section 6, we compare the three meshless methods for their accuracy and ease of implementation. In Section 7, we draw conclusions from the comparisons.

* Corresponding author.
E-mail address: chenwen@hhu.edu.cn (W. Chen).

0955-7997/$ - see front matter © 2010 Elsevier Ltd. All rights reserved.
doi:10.1016/j.enganabound.2010.03.004

2. Governing equations

For simplicity, we first consider the 2D case. We note that the formulation in this section can be easily extended to the 3D case. Let $\Omega \subset \mathbb{R}^2$. We consider the following differential equation:

$$\Delta^2 u(x,y)+\alpha(x,y)\frac{\partial u(x,y)}{\partial x}+\beta(x,y)\frac{\partial u(x,y)}{\partial y}+\gamma(x,y)u(x,y)=f(x,y) \quad (x,y)\in\Omega, \tag{1}$$

with Dirichlet boundary condition

$$u(x,y)=g(x,y) \quad (x,y)\in\partial\Omega, \tag{2}$$

and normal boundary condition

$$\frac{\partial u(x,y)}{\partial \mathbf{n}}=h_1(x,y)\cdot\mathbf{n} \quad (x,y)\in\partial\Omega, \tag{3}$$

or Laplace boundary condition

$$\Delta u(x,y)=h_2(x,y) \quad (x,y)\in\partial\Omega, \tag{4}$$

where Δ^2 denotes the biharmonic operator, Δ denotes the Laplace operator and $\partial/\partial\mathbf{n}$ is the normal derivative on the boundary $\partial\Omega$, α, β, γ, f, g, h_1, and h_2 are given functions. $\overline{\Omega}=\Omega\cup\partial\Omega$ is the computational domain.

3. The method of particular solutions

In the formulation of the MPS [12,18], the main idea is to rewrite (1) in the system as follows:

$$\Delta^2 u(x,y)=R\left(x,y,u,\frac{\partial u}{\partial x},\frac{\partial u}{\partial y}\right) \quad (x,y)\in\Omega, \tag{5}$$

where

$$R\left(x,y,u,\frac{\partial u}{\partial x},\frac{\partial u}{\partial y}\right)=-\alpha(x,y)\frac{\partial u(x,y)}{\partial x}-\beta(x,y)\frac{\partial u(x,y)}{\partial y}-\gamma(x,y)u(x,y)+f(x,y). \tag{6}$$

By keeping the biharmonic operator on the left-hand side as a main differential operator, the other terms have been moved to the right-hand side and treated as part of the forcing term. The right-hand side function is approximated by the radial basis functions as follows:

$$R\left(x,y,u,\frac{\partial u}{\partial x},\frac{\partial u}{\partial y}\right)=\sum_{j=1}^{n}\omega_j\phi(r_j), \tag{7}$$

where $r_j=\|(x,y)-(c_j,t_j)\|$, (c_j, t_j), $j=1, 2,\ldots,n$ are called the centers or trial points, and (x_j, y_j), $j=1, 2,\ldots,n$ are the centers. Note that $\omega_j, j=1,2,\ldots,n$ are the undetermined coefficients to be determined.

By repeating integration of radial basis function $\phi(r)$,

$$\Delta^2\Phi(r)=\phi(r), \tag{8}$$

the particular solution $\Phi(r)$ of biharmonic operator with right-hand side RBF $\phi(r)$ is obtained. Then, the exact solution can be approximated by

$$\hat{u}(x,y)=\sum_{j=1}^{n}\omega_j\Phi(r_j). \tag{9}$$

Thus,

$$\frac{\partial\hat{u}(x,y)}{\partial x}=\sum_{j=1}^{n}\omega_j\frac{\partial\Phi(r_j)}{\partial x},$$

$$\frac{\partial\hat{u}(x,y)}{\partial y}=\sum_{j=1}^{n}\omega_j\frac{\partial\Phi(r_j)}{\partial y},$$

$$\Delta^2\hat{u}(x,y)=\sum_{j=1}^{n}\omega_j\phi(r_j).$$

Thus, let $\{(x_j,y_j)\}_{j=1}^{n}$ be n distinct collocation points in $\overline{\Omega}$ of which $\{(x_j,y_j)\}_{j=1}^{n_i}$ are interior points and $\{(x_j,y_j)\}_{j=n_i+1}^{n}$ are boundary points. The biharmonic system with the normal boundary condition can be represented by a linear system

$$\sum_{j=1}^{n}\omega_j\left(\phi_j+\alpha\frac{\partial\Phi_j}{\partial x}+\beta\frac{\partial\Phi_j}{\partial y}+\gamma\Phi_j\right)(r_i)=f(x_i,y_i), \quad i=1,2,\ldots,n_i,$$

$$\sum_{j=1}^{n}\omega_j\Phi_j(r_i)=g(x_i,y_i), \quad i=n_i+1,\ldots,n,$$

$$\sum_{j=1}^{n}\omega_j\frac{\partial\Phi_j}{\partial\mathbf{n}}=h_1(x_i,y_i)\cdot\mathbf{n}, \quad i=n_i+1,\ldots,n. \tag{10}$$

By solving this linear system, $\{\omega_j\}_{j=1}^{n}$ can be obtained.

Next, we need to find the closed-form of the particular solution Φ in (8). In the 2D case,

(a) $\phi(r)=\sqrt{r^2+c^2}$, by direct integration, we have

$$\Psi(r)=\frac{4c^2+r^2}{9}\sqrt{r^2+c^2}-\frac{c^3}{3}\ln(c+\sqrt{r^2+c^2}), \tag{11}$$

where

$$\Delta\Psi(r)=\phi(r). \tag{12}$$

Since

$$\Delta\Phi(r)=\frac{\partial}{r\partial r}\left(\frac{\partial\Phi(r)}{\partial r}\right)=\Psi(r),$$

by direct integration,

$$\begin{aligned}\Phi(r)=&-\frac{7}{60}c^4\sqrt{r^2+c^2}+\frac{2}{45}c^2(r^2+c^2)^{3/2}+\frac{1}{225}(r^2+c^2)^{5/2}\\&+\frac{2c^2-5r^2}{60}c^3\ln(c+\sqrt{r^2+c^2})+\frac{1}{12}r^2c^3-\frac{c^5}{5}\ln(r)\\&+\frac{c^5}{30}\ln(2c)-\frac{1}{12}c^5+c_1,\end{aligned} \tag{13}$$

where c_1 is a constant. In (13), we notice that there is a singular term $\ln(r)$. Since $\Delta\ln(r)=0$, we have $\Delta^2\ln(r)=0$. This implies

$$\Delta^2\left(-\frac{c^5}{5}\ln(r)+\frac{c^5}{30}\ln(2c)-\frac{1}{12}c^5+c_1\right)=0.$$

We can remove the singular term and the constant terms in (13), i.e.,

$$\Delta^2\left[\Phi(r)-\left(-\frac{c^5}{5}\ln(r)+\frac{c^5}{30}\ln(2c)-\frac{1}{12}c^5+c_1\right)\right]=\phi(r).$$

Hence,

$$\begin{aligned}\Phi(r)=&-\frac{7}{60}c^4\sqrt{r^2+c^2}+\frac{2}{45}c^2(r^2+c^2)^{3/2}+\frac{1}{225}(r^2+c^2)^{5/2}\\&+\frac{2c^2-5r^2}{60}c^3\ln(c+\sqrt{r^2+c^2})+\frac{1}{12}r^2c^3\end{aligned} \tag{14}$$

is a particular solution of biharmonic operator using MQ as a radial basis function. Note that the particular solution is not unique. We have the freedom to choose any particular solution Φ as long as Φ satisfies (8). It follows that

$$\begin{aligned}\frac{1}{r}\frac{\partial\Phi(r)}{\partial r}=&-\frac{7}{60}\frac{c^4}{\sqrt{r^2+c^2}}+\frac{2c^2}{15}\sqrt{r^2+c^2}+\frac{1}{45}(r^2+c^2)^{3/2}+\frac{1}{6}c^3\\&+\frac{(2c^2-5r^2)c^3}{60\sqrt{r^2+c^2}\ln(c+\sqrt{r^2+c^2})}-\frac{c^3}{6}\ln(c+\sqrt{r^2+c^2}).\end{aligned} \tag{15}$$

Eq. (15) is required in the evaluation of normal derivative on the boundary.

(b) $\phi(r)=r^{2n-1}$, we have

$$\Phi(r)=\frac{r^{2n+3}}{(2n+1)^2(2n+3)^2}. \tag{16}$$

In the 3D case, the closed-form of the particular solution Φ is not available for $\phi=\sqrt{r^2+c^2}$. For $\phi(r)=r^{2n-1}$, we have

$$\Phi(r)=\frac{r^{2n+3}}{(2n+1)(2n+2)(2n+3)(2n+4)}. \tag{17}$$

4. The MFS-MPS

In this section, we briefly introduce the one-stage technique of the newly developed MFS-MPS [1]. Based on the idea that the solutions of a given partial differential equation can be written as the sum of a particular solution and its associated homogeneous solution, we assume the solution of (1)–(4) can be written in the following form:

$$\hat{u}(x,y)=\sum_{i=1}^{n_i}\omega_i\Phi(r_i)+\sum_{j=1}^{n_b}\mu_j G(\rho_j), \tag{18}$$

where $\Phi(r)$ is defined the same as (8), and $\rho_i=\|(x,y)-(c_i,t_i)\|$. Note that $(c_i,\ t_i)$, $i=1,\ 2,\ \ldots,\ n_b$ are source points on the fictitious boundary outside the domain. We also observe that

$$\Delta^2 G(\rho)=0, \tag{19}$$

since $\rho\neq 0$. From (18), it follows that

$$\frac{\partial\hat{u}(x,y)}{\partial x}=\sum_{i=1}^{n_i}\omega_i\frac{\partial\Phi(r_i)}{\partial x}+\sum_{j=1}^{n_b}\mu_j\frac{\partial G(\rho_j)}{\partial x},$$

$$\frac{\partial\hat{u}(x,y)}{\partial y}=\sum_{i=1}^{n_i}\omega_i\frac{\partial\Phi(r_i)}{\partial y}+\sum_{j=1}^{n_b}\mu_j\frac{\partial G(\rho_j)}{\partial y},$$

$$\Delta\hat{u}(x,y)=\sum_{i=1}^{n_i}\omega_i\Delta\Phi(r_i)+\sum_{j=1}^{n_b}\mu_j\Delta G(\rho_j),$$

$$\Delta^2\hat{u}(x,y)=\sum_{i=1}^{n_i}\omega_i\phi(r_i).$$

For instance, for the given differential equation (1) with boundary conditions (2) and (4), the weights $\omega=[\omega_1\ \omega_2\ldots\omega_{n_i}]^T$ and $\mu=[\mu_1\ \mu_2\ldots\mu_{n_b}]^T$ can be determined by solving the following linear system:

$$\sum_{j=1}^{n_i}\omega_j\left(\phi_j+\alpha\frac{\partial\Phi_j}{\partial x}+\beta\frac{\partial\Phi_j}{\partial y}+\gamma\Phi_j\right)(r_i)+\sum_{j=1}^{n_b}\mu_j\left(\alpha\frac{\partial G_j}{\partial x}+\beta\frac{\partial G_j}{\partial y}+\gamma G_j\right)(\rho_i)=f(x_i,y_i),\quad i=1,2,\ldots,n_i,$$

$$\sum_{j=1}^{n_i}\omega_j\Phi_j(r_i)+\sum_{j=1}^{n_b}\mu_j G_j(\rho_i)=g(x_i,y_i),\quad i=n_i+1,\ldots,n,$$

$$\sum_{j=1}^{n_i}\omega_j\Delta\Phi_j(r_i)+\sum_{j=1}^{n_b}\mu_j\Delta G_j(\rho_i)=h_2(x_i,y_i),\quad i=n_i+1,\ldots,n.$$

Rewriting in matrix notation, we have that

$$\begin{bmatrix}\phi+\alpha\Phi_x+\beta\Phi_y+\gamma\Phi & \alpha G_x+\beta G_y+\gamma G\\ \Phi & G\\ \Delta\Phi & \Delta G\end{bmatrix}\begin{bmatrix}\omega\\ \mu\end{bmatrix}=\begin{bmatrix}f\\ g\\ h_2\end{bmatrix}. \tag{20}$$

In this paper, the main differential operator is Δ^2 and its fundamental solution is given as follows:

$$G(\rho)=\begin{cases}\rho^2\ln(\rho) & \text{in 2D},\\ \rho & \text{in 3D}.\end{cases} \tag{21}$$

For the over-determined system (20), we can obtain all weights ω and μ using the least square method. Instead of finding a particular solution and its associated homogeneous solution separately, the above formulation allows us to obtain the solution in one step. Furthermore, such an approach makes it possible for the MFS to solve elliptic partial differential equations with variable coefficients.

5. Kansa's method

Kansa's method is a well-known meshless method using radial basis functions. For completeness, we briefly introduce the method in this section.

Let $\{(x_j,y_j)\}_{j=1}^{n}$ be n distinct collocation points in $\overline{\Omega}$ of which $\{(x_j,y_j)\}_{j=1}^{n_i}$ are interior points and $\{(x_j,y_j)\}_{j=n_i+1}^{n}$ are boundary points.

The main idea of Kansa's method is to approximate the solution u by the linear combination of radial basis functions, i.e.,

$$\hat{u}(x,y)=\sum_{j=1}^{n}\omega_j\phi_j(r), \tag{22}$$

where $\{\omega_j\}_{j=1}^{n}$ are coefficients to be determined. From (1), (2) and (4), we have

$$\sum_{j=1}^{n}\omega_j\left(\Delta^2\phi_j+\alpha\frac{\partial\phi_j}{\partial x}+\beta\frac{\partial\phi_j}{\partial y}+\gamma\phi_j\right)(r_i)=f(x_i,y_i),\quad i=1,2,\ldots,n_i,$$

$$\sum_{j=1}^{n}\omega_j\phi_j(r_i)=g(x_i,y_i),\quad i=n_i+1,\ldots,n,$$

$$\sum_{j=1}^{n}\omega_j\Delta\phi_j(r_i)=h_2(x_i,y_i),\quad i=n_i+1,\ldots,n, \tag{23}$$

which is an over-determined system and the unknowns $\{\omega_j\}_{j=1}^{n}$ can be obtained by least square method. In general, MQ is one of the most widely adopted RBFs in Kansa's method.

Note that the formulation of the MPS and Kansa's method is similar. The linear systems (10) and (23) are exactly the same, but Kansa's method uses the RBF $\phi(r)$ directly, and the MPS uses the particular solution of biharmonic operator with chosen right-hand side RBF. The choice of basis functions for Kansa's method is ad hoc. The derivation of the basis function for the MPS is more rigorous. The MPS evolved from the MFS-MPS but end up similar to Kansa's method. In some sense, these methods are closely related.

6. Numerical results

To make a comparison of the effectiveness among three numerical methods mentioned in the previous sections, three numerical examples are given. Through all the numerical tests in this section, we use the following formula to choose the location of the source points in the MFS-MPS:

$$\mathbf{x}^s=\mathbf{x}^b+d(\mathbf{x}^b-\mathbf{x}^c), \tag{24}$$

where $\mathbf{x}_s$, $\mathbf{x}_b$, and $\mathbf{x}_c$ denote the source, boundary, and central nodes respectively. d determines how far the source points from the boundary. The distribution of interpolation points in Ω, boundary collocation points on $\partial\Omega$, and source points on Γ are

shown in Fig. 1. In the rest of the section, n_i is denoted as the number of the interior points and n_b the number of boundary points.

To validate the numerical accuracy, we calculate the following root mean square errors, RMSE and RMSEx:

$$\varepsilon = \mathrm{RMSE} = \sqrt{\frac{1}{q}\sum_{j=1}^{q}(\hat{u}_j - u_j)}, \tag{25}$$

$$\varepsilon_x = \mathrm{RMSE}x = \sqrt{\frac{1}{q}\sum_{j=1}^{q}\left(\frac{\partial \hat{u}_j}{\partial x} - \frac{\partial u_j}{\partial x}\right)}, \tag{26}$$

where q is the number of testing nodes chosen randomly in the domain. $\hat{u}_j$ denotes the approximate solution at the j-th node. To save space we do not show the numerical results of RMSEy since it is similar to RMSEx.

In the next three examples, we compare the numerical results in terms of accuracy for solving higher-order elliptic equations using three different methods discussed in the previous sections. We use the well-known Golden Section Search Algorithm [15] to find a reasonable choice of shape parameter c of MQ and an acceptable d in (24).

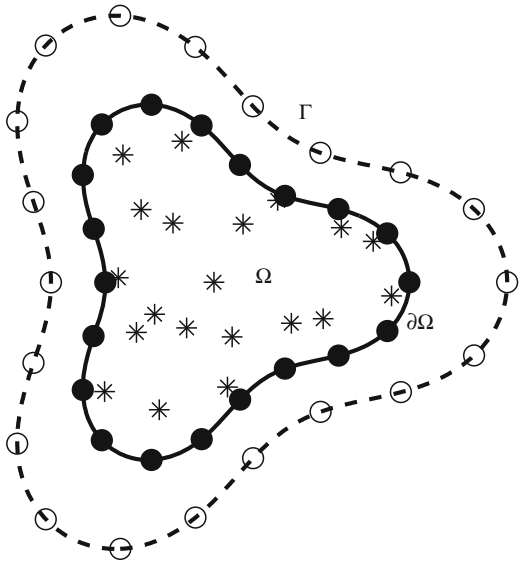

Fig. 1. Interpolation points (∗), boundary collocation points (•), and source points (◦) on the fictitious boundary.

Example 1. We consider the following partial differential equation:

$$\Delta^2 u(x,y) + x^2y^3u(x,y) + y\cos(y)\frac{\partial u}{\partial x}(x,y) + \sinh(x)\frac{\partial u}{\partial y}(x,y) = f(x,y) \quad (x,y)\in\Omega,$$

$$u(x,y) = \sin(\pi x)\cosh(y) - \cos(\pi x)\sinh(y) \quad (x,y)\in\partial\Omega,$$

$$\frac{\partial u}{\partial \mathbf{n}}(x,y) = g(x,y)\cdot\mathbf{n} \quad (x,y)\in\partial\Omega,$$

where $f(x,y)$ and $g(x,y)$ are generated from the following analytical solution:

$$u(x,y) = \sin(\pi x)\cosh(y) - \cos(\pi x)\sinh(y) \quad (x,y)\in\overline{\Omega}. \tag{27}$$

The computational domain is bounded by Cassini curve which is defined by the following parametric equation:

$$\partial\Omega = \{(x,y)|x = \rho\cos\theta, y = \rho\sin\theta,\ 0\le\theta\le 2\pi\}, \tag{28}$$

where

$$\rho = \left(\cos(3\theta) + \sqrt{2-\sin^2(3\theta)}\right)^{1/3}. \tag{29}$$

The computational domain and profile of the exact solution in the extended domain are depicted in Fig. 2. We choose 256 testing points for the evaluation of RMSE and RMSEx. In Tables 1 and 2, we compare the results of RMSE and RMSEx for three different methods using MQ. We observe that the MFS-MPS performs one order of magnitude better than the MPS and Kansa's method. There is little difference between the MPS and Kansa's method. Moreover, the accuracy is improving quickly as increasing the number of interior and boundary nodes.

RMSEx is one order of magnitude less accurate than the RMSE as shown in the table. In particular, if we replace MQ by the basis functions $\phi(r) = r^{2n-1}$, then the MPS is identical to Kansa's

Table 1
Results of RMSE for MPS, MFS-MPS, and Kansa's method using MQ.

(n_i,n_b)	MPS		MFS-MPS			Kansa's method	
	ε	c	ε	c	d	ε	c
(60,30)	1.36E−3	1.46	2.13E−3	3.17	9.55	1.33E−3	3.27
(126,60)	8.21E−4	0.71	1.24E−4	2.13	5.05	8.46E−4	2.23
(208,90)	3.51E−4	0.62	1.38E−4	1.45	7.21	7.09E−4	1.07
(310,120)	2.30E−4	0.40	7.17E−5	1.00	3.63	6.98E−4	0.93
(406,150)	2.29E−4	0.45	7.04E−5	1.28	3.85	7.09E−4	0.69
(507,180)	3.35E−4	0.31	6.25E−5	1.06	3.82	7.12E−4	0.59

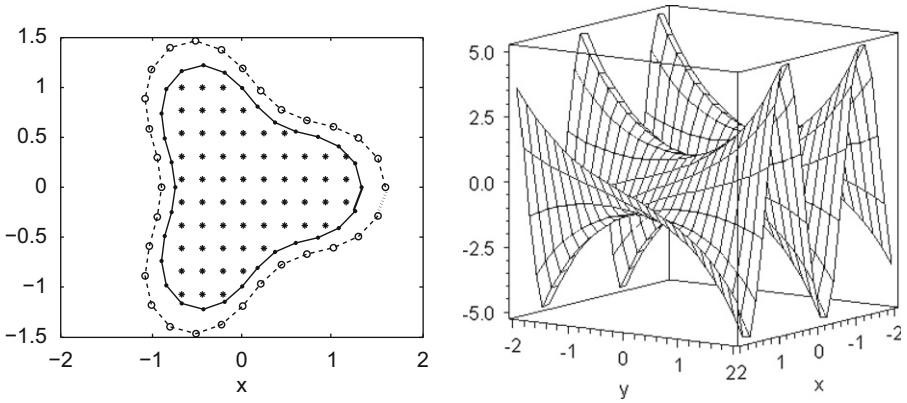

Fig. 2. The computational domain (left) and profile of the solution in the extended domain (right).

Table 2
Results of RMSEx for MPS, MFS-MPS, and Kansa's method using MQ.

(n_i,n_b)	ε_x		
	MPS	MFS-MPS	Kansa's method
(60,30)	5.71E−3	9.67E−3	5.52E−3
(126, 60)	4.33E−3	7.18E−4	3.10E−3
(208,90)	2.83E−3	7.78E−4	2.50E−3
(310,120)	2.51E−3	5.18E−4	2.38E−3
(406,150)	4.62E−3	4.46E−4	2.79E−3
(507,180)	3.06E−3	4.26E−4	3.00E−3

Table 3
Results of RMSE and RMSEx using RBF $\phi(r)=r^5$.

(n_i, n_b)	MPS		MFS-MPS		
	ε	ε_x	ε	ε_x	d
(60,30)	4.85E−2	1.98E−1	3.54E−3	1.64E−2	9.55
(126,60)	4.57E−3	3.54E−2	6.04E−4	3.76E−3	3.89
(208,90)	1.46E−3	1.12E−2	1.47E−4	9.82E−4	3.89
(310,120)	4.45E−4	3.51E−3	1.51E−4	9.84E−4	4.03
(310,160)	5.19E−4	3.97E−3	1.59E−4	1.01E−3	4.00
(406,120)	5.99E−4	3.98E−3	1.66E−4	1.07E−3	4.10
(406,160)	6.78E−4	4.71E−3	1.35E−4	8.75E−4	4.50
(507,160)	7.03E−4	4.67E−3	1.63E−4	1.04E−3	4.43
(507,200)	4.40E−4	3.20E−3	3.64E−4	2.34E−3	3.08

Table 4
RMSE and RMSEx for the MPS using different orders of RBF $\phi(r)=r^{2n-1}$ and different numbers of interior and boundary points.

n	n_i=310, n_b=120		n_i=406, n_b=160	
	ε	ε_x	ε	ε_x
1	6.54E−3	3.70E−2	3.78E−3	1.91E−2
2	8.35E−4	4.73E−3	4.53E−4	1.71E−3
3	4.45E−4	3.51E−3	6.78E−4	4.71E−3
4	3.42E−4	1.94E−3	3.35E−4	2.13E−3

method. In Table 3, we use $\phi(r)=r^5$ and observe that the MFS-MPS performs slightly better than the MPS. For the MPS as shown in Table 3, we do not have to worry about finding a good shape parameter and the location of the source points since the MFS is not required in the solution process.

In Table 4, we show the RMSE and RMSEx for the MPS using $\phi(r)=r^{2n-1}$ for various order of n. There is a clear difference in accuracy between $n=1$ and 2 and little improvement when $n>2$.

Example 2. Next, we consider the following convection–diffusion equation:

$$\Delta^2 u(x,y)+xyu(x,y)+2y\sin x\frac{\partial u}{\partial x}(x,y)-y\cos x\frac{\partial u}{\partial y}(x,y)=f(x,y)\quad (x,y)\in\Omega,$$

$$u(x,y)=y\sin x+x\cos y\quad (x,y)\in\partial\Omega,$$

$$\Delta u(x,y)=g(x,y)\quad (x,y)\in\partial\Omega,$$

where $f(x,y)$ and $g(x,y)$ are generated from the following analytical solution:

$$u(x,y)=y\sin x+x\cos y\quad (x,y)\in\overline{\Omega}. \tag{30}$$

The domain is bounded by the following peanut shape parametric curve:

$$\partial\Omega=\{(x,y)|x=\rho\cos\theta,y=\rho\sin\theta,0\le\theta\le 2\pi\},$$

where

$$\rho=\left(\cos(2\theta)+\sqrt{1.1-\sin^2(2\theta)}\right).$$

The profiles of the computational domain and the exact solution in the extended domain are shown in Fig. 3.

In Tables 5 and 6, we show the results of the RMSE and RMSEx using MQ for different numbers of points both in the domain and on the boundary for three methods: the MPS, MFS-MPS, and Kansa's method. It shows that the number of interior points and boundary collocation points has little effect on the accuracy of the solution. We notice that with small number of interior and boundary points, we can achieve high accuracy. Similar to the results in Example 1, the MFS-MPS consistently outperforms the MPS and Kansa's method. We also observe that the MPS performs one order of magnitude better than Kansa's method in the evaluation of RMSE and RMSEx.

Example 3. In this example, we consider the three dimensional problem

$$\Delta^2 u+\alpha u+\beta\frac{\partial u}{\partial x}+\gamma\frac{\partial u}{\partial y}+\delta\frac{\partial u}{\partial z}=f(x,y,z)\quad (x,y,z)\in\Omega,$$

$$u=\tfrac{1}{120}(x^5+y^5+z^5)\quad (x,y,z)\in\partial\Omega,$$

$$\Delta u=g(x,y,z)\quad (x,y,z)\in\partial\Omega,$$

where

$$\alpha=\sinh(x)\cos(y)\sin(z),$$

$$\beta=x^3\sin(y)e^z,$$

$$\gamma=-\cos(x)\cosh(y)\cos(z),$$

$$\delta=\tfrac{1}{20}e^x\sin(y)\tan(z).$$

The non-homogeneous terms $f(x,y,z)$ and $g(x,y,z)$ are generated from the following analytical solution:

$$u(x,y,z)=\tfrac{1}{120}(x^5+y^5+z^5)\quad (x,y,z)\in\overline{\Omega}. \tag{31}$$

Let

$$R(\theta)=\sqrt{\cos(2\theta)+\sqrt{1.1-\sin^2(2\theta)}}.$$

The surface of the computational domain is represented by following parametric equation:

$$r(\theta,\phi)=R(\theta)\cos(\theta)\mathbf{i}+R(\theta)\sin(\theta)\cos(\phi)\mathbf{j}+R(\theta)\sin(\theta)\sin(\phi)\mathbf{k}, \tag{32}$$

where $\theta\in[0,\pi),\phi\in[0,2\pi)$. The profile of the domain is shown in Fig. 4.

In this example, 82 uniform grids are chosen as testing nodes for calculating the *RMSE*, *RMSEx*, and $RMSE_\Delta$, where

$$RMSE_\Delta=\sqrt{\frac{1}{q}\sum_{j=1}^{q}(\Delta\hat{u}(x_j,y_j,z_j)-\Delta u(x_j,y_j,z_j))^2}. \tag{33}$$

Furthermore, we choose r^{2n-1} as the basis functions. In this case, the MPS and Kansa's method are identical. Hence, in this example we only compare the results of the MPS and MFS-MPS. From Table 7, we choose r^5 as the basis function with various number of interior and boundary points. The accuracy is increasing quickly as increasing the number of collocation nodes, but becomes stable

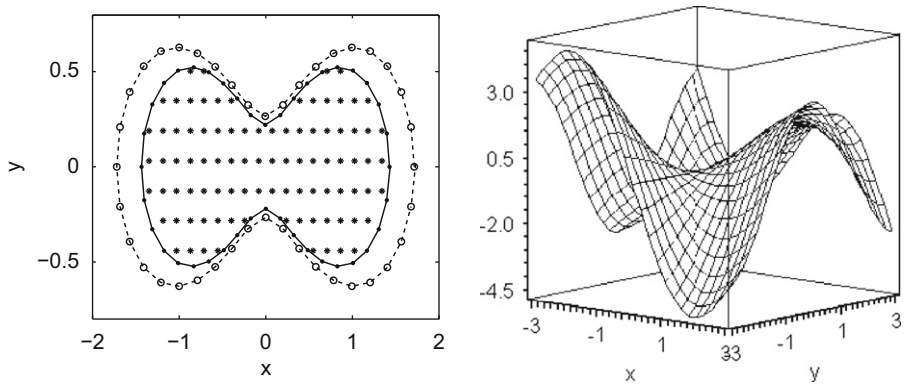

Fig. 3. The profiles of the computational domain (left) and the solution in the extended domain (right).

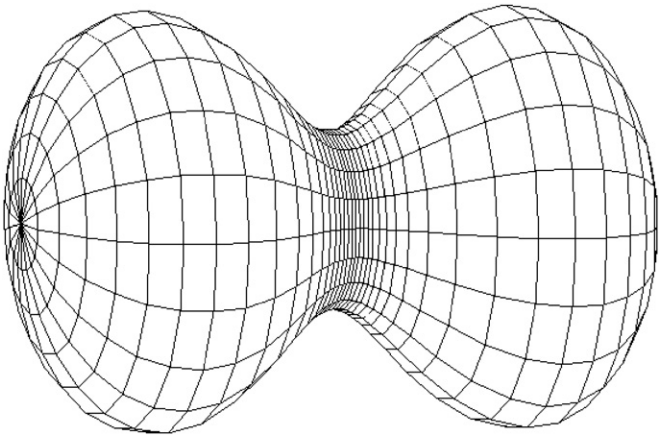

Fig. 4. Peanut-shape computational domain.

Table 5
RMSE of the MPS, MFS-MPS, and Kansa's method using MQ with corresponding parameters c and d.

(n_i,n_b)	MPS		MFS-MPS			Kansa's method	
	ε	c	ε	c	d	ε	c
(25,20)	7.03E−5	6.41	3.97E−5	5.34	3.87	1.15E−3	6.17
(86,40)	1.71E−5	4.37	3.67E−6	2.37	3.80	2.16E−4	4.53
(145,60)	2.04E−5	3.99	1.19E−6	4.00	4.59	9.46E−4	4.58
(190,80)	1.51E−5	3.86	1.77E−6	3.29	3.24	5.21E−4	4.18
(250,100)	2.63E−5	4.39	1.52E−6	4.00	5.28	6.01E−4	3.73
(293,120)	5.49E−5	4.71	2.02E−6	3.14	3.64	9.62E−4	5.96

Table 6
RMSEx of the MPS, MFS-MPS, and Kansa's method using MQ.

(n_i,n_b)	ε_x		
	MPS	MFS-MPS	Kansa's method
(25,20)	3.74E−4	2.52E−4	2.96E−3
(86,40)	1.03E−4	2.54E−5	1.84E−3
(145,60)	1.28E−4	1.20E−5	3.19E−3
(190,80)	1.14E−4	1.18E−5	3.48E−3
(250,100)	1.56E−4	1.28E−5	2.11E−3
(293,120)	3.26E−4	1.45E−5	5.26E−3

Table 7
RMSE and *RMSEx* obtained by different number of interpolation nodes and the order of RBFs is $n=3$.

(n_i, n_b)	MPS		MFS-MPS		
	ε	ε_x	ε	ε_x	d
(42,24)	2.99E−3	1.07E−2	5.14E−4	2.58E−3	1.89
(128,60)	1.43E−3	6.63E−3	9.70E−5	2.10E−3	1.90
(232,98)	1.09E−4	2.44E−4	5.88E−5	1.50E−3	1.65
(350,144)	7.43E−5	1.52E−4	5.36E−5	2.89E−3	2.72
(538,220)	5.06E−5	1.68E−4	6.78E−5	1.70E−3	2.23
(632,300)	5.09E−5	1.60E−4	5.10E−5	2.09E−3	2.03

Table 8
RMSE and *RMSEx* obtained using different order of RBFs, where $n_i=538$, $n_b=220$.

	RMSE		RMSEx	
	MPS	MFS-MPS	MPS	MFS-MPS
r^5	5.06E−5	6.78E−5	1.68E−4	1.70E−3
r^7	5.03E−5	5.17E−5	1.61E−4	1.44E−3
r^9	4.95E−5	4.58E−5	1.51E−4	6.63E−4
r^{11}	5.37E−5	5.00E−5	1.90E−4	1.95E−3

after enough large amount of nodes is used. Such an attractive feature is very desirable in the numerical computation. The results in Table 8 are produced using 538 interior points and 220 boundary points. We observe little difference using different basis functions.

7. Conclusions

In this paper we make a comparison among three meshless methods using radial basis functions. The one-stage MFS-MPS was recently developed, and then followed by the MPS. In these two approaches, the particular solution and/or the fundamental solution are required for solving partial differential equations. The third method is Kansa's method which is well known in the meshless literature. In all the numerical comparisons shown in the last section, the MFS-MPS performs the best, followed by the MPS and then Kansa's method. On the other hand, it is interesting to note the ranking of easiness in implementation of these three methods is reversed. The MFS-MPS requires the fundamental solution and derivation of the particular solution. The determination of the optimal source location is not trivial. Both the MFS-MPS and the

MPS require the closed-form of the particular solution using RBFs. However, not all the closed-form of the particular solution is available. For instance, the closed-form of the particular solution using MQ for the 3D case in Example 3 is not available. Hence, Kansa's method is the easiest method in term of numerical implementation.

References

[1] Chen CS, Fan CM, Monroe J. The method of fundamental solutions for solving elliptic pdes with variable coefficients. In: Chen CS, Karageorghis A, Smyrlis YS, editors. The method of fundamental solutions—a meshless method. Atlanta: Dynamic Publishers; 2008. p. 75–105.

[2] Chen W, Tanaka M. New insights into boundary-only and domain-type RBF methods. Int J Nonlinear Sci Numer Simulation 2000;1:145–51.

[3] Chen W, Tanaka M. A meshless, exponential convergence, integration-free, and boundary-only RBF technique. Comput Math Appl 2002;43:379–91.

[4] Cheng AH-D. Particular solutions of Laplacian, Helmholtz-type, and polyharmonic operators involving higher order radial basis functions. Eng Anal Boundary Elem 2000;24:531–8.

[5] Cheng AH-D, Ahtes H, Ortner N. Fundamental solutions of product of Helmholtz and polyharmonic operators. Eng Anal Boundary Elem 1994;14:187–91.

[6] Cheng AH-D, Morohunfola OK. Multilayered leaky aquifer systems: I. Pumping well solution. Water Resources Res 1993;29:2787–800.

[7] Cheng AH-D, Morohunfola OK. Multilayered leaky aquifer systems: II. Boundary element solution. Water Resources Res 1993;29:2801–11.

[8] Golberg MA, Chen CS. The method of fundamental solutions for potential, Helmholz and diffusion problems. In: Golberg MA, editor. Boundary integral methods: numerical and mathematical aspects. Boston: WIT Press, Computational Mechanics Publications; 1998. p. 103–176.

[9] Hömander L. Linear partial differential operators. Berlin: Springer; 1963.

[10] Kansa EJ. Multiquadrics—a scattered data approximation scheme with applications to computational fluid dynamics—II. Comput Math Appl 1990;19:147–61.

[11] Karageorghis A, Fairweather G. The method of fundamental solutions for axisymmetric acoustic scattering and radiation problems. J Acoust Soc Am 1998;104:3212–8.

[12] Katsikadelis JT. The 2D elastostatic problem in inhomogeneous anisotropic bodies by the meshless analog equation method (MAEM). Eng Anal Boundary Elem 2008;32:997–1005.

[13] Li J, Hon YC, Chen CS. Numerical comparisons of two meshless methods using radial basis functions. Eng Anal Boundary Elem 2002;26:205–25.

[14] Myers TG, Charpin JPF. A mathematical model for atmospheric ice accretion and water flow on a cold surface. Int J Heat Mass Transfer 2004;47:5483–500.

[15] Press WH, Teukolsky SA, Vetterling WT, Flannery BP. Numerical recipes in fortran: the art of scientific computing, 3rd ed. New York, NY, USA: Cambridge University Press; 2007.

[16] Tsai CC, Cheng AH-D, Chen CS. Particular solutions of splines and monomials for polyharmonic and products of Helmholtz operators. Eng Anal Boundary Elem 2009;33:514–21.

[17] Wang H, Qin QH. A meshless method for generalized linear or nonlinear poisson-type problems. Eng Anal Boundary Elem 2006;30:515–21.

[18] Wen PH, Chen CS. The method of particular solution for solving scalar wave equations. Int J Numer Methods Biomed Eng 2010;9999:2040–7939.